

FULL REGENERATION OF SEGMENTAL BONE DEFECTS USING POROUS TITANIUM IMPLANTS LOADED WITH BMP-2 CONTAINING FIBRIN GELS

J. van der Stok^{1*}, M.K.E. Koolen^{1,2}, M.P.M. de Maat³, S. Amin Yavari⁴, J. Alblas², P. Patka⁵, J.A.N. Verhaar¹, E.M.M. van Lieshout⁶, A.A. Zadpoor⁴, H. Weinans^{2,4,7} and H. Jahr⁸

¹Orthopaedic Research Laboratory, Department of Orthopaedics, Erasmus University, Medical Centre Rotterdam, Rotterdam, The Netherlands

²Department of Orthopaedics, University Medical Centre Utrecht, Utrecht, The Netherlands

³Department of Haematology, Erasmus University Medical Centre Rotterdam, Rotterdam, The Netherlands

⁴Department of Biomechanical Engineering, Delft University of Technology, Delft, The Netherlands

⁵Department of Emergency Medicine, Department of Orthopaedics, Erasmus University Medical Centre Rotterdam, Rotterdam, The Netherlands

⁶Trauma Research Unit, Department of Surgery, Erasmus University Medical Centre Rotterdam, Rotterdam, The Netherlands

⁷Department of Rheumatology, University Medical Centre Utrecht, Utrecht, The Netherlands

⁸Department of Orthopaedics Surgery, University Hospital RWTH Aachen, Aachen, Germany

Abstract

Regeneration of load-bearing segmental bone defects is a major challenge in trauma and orthopaedic surgery. The ideal bone graft substitute is a biomaterial that provides immediate mechanical stability, while stimulating bone regeneration to completely bridge defects over a short period. Therefore, selective laser melted porous titanium, designed and fine-tuned to tolerate full load-bearing, was filled with a physiologically concentrated fibrin gel loaded with bone morphogenetic protein-2 (BMP-2). This biomaterial was used to graft critical-sized segmental femoral bone defects in rats. As a control, porous titanium implants were either left empty or filled with a fibrin gels without BMP-2. We evaluated bone regeneration, bone quality and mechanical strength of grafted femora using *in vivo* and *ex vivo* μ CT scanning, histology, and torsion testing. This biomaterial completely regenerated and bridged the critical-sized bone defects within eight weeks. After twelve weeks, femora were anatomically re-shaped and revealed open medullary cavities. More importantly, new bone was formed throughout the entire porous titanium implants and grafted femora regained more than their innate mechanical stability: torsional strength exceeded twice their original strength. In conclusion, combining porous titanium implants with a physiologically concentrated fibrin gels loaded with BMP-2 improved bone regeneration in load-bearing segmental defects. This material combination now awaits its evaluation in larger animal models to show its suitability for grafting load-bearing defects in trauma and orthopaedic surgery.

Keywords: BMP, bone graft, bone regeneration, fibrin, metal surface treatment, scaffold, titanium.

*Address for correspondence:

Johan van der Stok, MD

Room Ee1614, PO Box 2040, 3000 CA Rotterdam, The Netherlands

Telephone number: +31-10-7043384

Fax number: +31-10-7044690

E-mail: j.vanderstok@erasmusmc.nl

Introduction

A major challenge in trauma and orthopaedic surgery is to successfully repair load-bearing segmental bone defects (Einhorn, 1995). This often requires the use of bone grafts or bone graft substitutes to improve bone regeneration by providing an osteoconductive matrix, offering mechanical support, or an osteoinductive and/or osteogenic stimulus (Giannoudis *et al.*, 2011). The golden standard bone graft is still autologous bone (Pape *et al.*, 2010), but the amount of bone that can be harvested is limited and associated with complications in 10-40 % (Banwart *et al.*, 1995). These disadvantages motivate the development of biomaterials that can be used as bone graft substitutes (Langer and Vacanti, 1993).

A biomaterial that has the potential to become a bone graft substitute is porous titanium (Alvarez and Nakajima, 2009; Murr *et al.*, 2010; Ryan *et al.*, 2006). Nowadays, porous titanium can be manufactured using additive manufacturing techniques such as selective laser melting (SLM) (Hollander *et al.*, 2006). This enables the design of porous titanium so that its structure and mechanical strength remains suitable to function as a load-bearing osteoconductive matrix in segmental bone defects (Van der Stok *et al.*, 2013a). Osseointegration of titanium is optimised through relatively simple chemical and heat treatments that alter the surface chemistry and (nano-) topography (Amin Yavari *et al.*, 2014a). Thereby, the bioinert titanium surface changes into a bioactive surface that allows spontaneous apatite formation and stimulates proliferation and osteogenic differentiation of osteoprogenitor cells (Amin Yavari *et al.*, 2014b). This surface-treated porous titanium forms a load-bearing osteoconductive matrix, but stimulating bone regeneration and adequate bridging of segmental bone defects may be further improved by addition of effective biological stimuli (*i.e.* osteoinductive cytokines) (de Wild *et al.*, 2013; Van der Stok *et al.*, 2013a).

Bone morphogenetic proteins (BMPs) such as BMP-2 and BMP-7 play a major role in bone regeneration as osteoinductive cytokines (Urist, 1965). Their osteoinductive effects have been established in a wide range of species,

varying from mice and rats to humans (Murakami *et al.*, 2002). BMP-2 and BMP-7 have received USA Food and Drugs Administration (FDA) approval for use in trauma and orthopaedic surgery (Senta *et al.*, 2009), but their clinical success is limited (Khan and Lane, 2004). This might be because a supra-physiological dosage of BMP needs to be loaded onto an absorbable collagen sponge to reach an effect (Termaat *et al.*, 2005). This high dose has been associated with adverse effects including bone tissue overgrowth, ectopic bone formation, inflammation, and even carcinogenicity (Carragee *et al.*, 2011; Woo, 2013). To overcome this, numerous slow-release systems have been developed. Interestingly, these slow-release systems, allowing for controlled release of BMP-2 during several weeks, do not resemble the natural bone regeneration process in which BMP-2 is mainly released during the first few days (Cho *et al.*, 2002; Gerstenfeld *et al.*, 2003).

Bone regeneration starts with the formation of a fibrin clot, often referred to as the fracture haematoma. This fibrin clot forms the natural binding reservoir for osteoinductive cytokines such as BMP-2 (Gerstenfeld *et al.*, 2003; Martino *et al.*, 2013) and is formed through conversion of fibrinogen by thrombin. Fibrinogen is synthesised in its high molecular weight form, but occurs as a mixture together with partially degraded low molecular weight forms in circulation (Kaijzel *et al.*, 2006). Fibrin gels, made from physiological fibrinogen concentrations (2–4 mg/L), are highly permeable to cells (Kaijzel *et al.*, 2006). However, at these physiological concentrations, fibrin gels are soft and therefore not suitable for most clinical applications. Consequently, commercially available fibrin sealants contain very high fibrinogen concentrations (50–100 mg/L) (Janmey *et al.*, 2009) at the cost of seriously compromising the favourable cellular permeability of these gels. When incorporated into porous titanium, the use of physiologically concentrated fibrin gels becomes feasible as the metal frame ensures mechanical support, then. The surface-treated porous titanium implants may even improve the network organisation of fibrin fibres (Milleret *et al.*, 2011).

The aim of the current study was to develop a biomaterial capable of improving bone regeneration of segmental bone defects: osteoconductive load-bearing porous titanium filled with physiologically concentrated fibrin gels releasing BMP-2. For this novel combination, the BMP-2 releasing fibrin gel was prepared from purified high molecular weight (HMW) fibrinogen, since HMW fibrinogen increases angiogenesis *in vitro* and *in vivo*. (Kaijzel *et al.*, 2006). To determine whether the angiogenic HMW fibrin gel alone is capable of increasing bone regeneration, porous titanium implants were also filled with HMW fibrin gels without BMP-2 and compared to unfractionated (UNF) fibrin gels. Porous titanium implants incorporated with the three above described fibrin gels were compared to empty porous titanium implants in a critical-sized load-bearing segmental femur defect in rats using *in vivo* (4, 8 and 12 weeks) and *ex vivo* (after 12 weeks) μ CT scans, histology, and biomechanical torsion tests.

Materials and Methods

Porous titanium implants

Porous titanium implants were produced from Ti6Al4V ELI powder (ASTM B348, grade 23) using selective laser melting (SLM, Layerwise N.V., Leuven, Belgium). The implants were a copy of the replaced femoral bone segment and had a height of 6 mm, a maximum outer diameter of 5 mm and a minimal inner diameter of 1.3 mm (leaving an open medullary canal). The porous architecture was based on a dodecahedron unit cell with a strut width of 120 μ m and an average pore size of 500 μ m, to result in 55 mm³ porous volume. All implants underwent a post-production alkali-acid-heat treatment consisting of (1) immersion in a 5 M aqueous NaOH solution at 60 °C for 24 h; (2) immersion in water at 40 °C for 24 h; (3) immersion in 0.5 mM HCl at 40 °C for 24 h; (4) heating to 600 °C at a rate of 5 °C/min in an electric furnace at ambient air pressure, keeping the temperature at 600 °C for 1 h, and subsequent natural cooling (Amin Yavari *et al.*, 2014b). Reproducibility of porous implant architecture (*e.g.*, pore size, titanium strut thickness and porosity) was verified by μ CT (SkyScan 1076; Bruker micro-CT N.V., Kontich, Belgium).

Fibrin gel preparation

Fibrin gel preparation was done as previously described (Holm *et al.*, 1985; Kaijzel *et al.*, 2006). Briefly, plasminogen-rich unfractionated human fibrinogen (Chromogenix, Mölndal, Sweden) was dissolved in Tris buffer (10 mM Tris/HCl, pH 7.4) to a concentration of 5 mg/mL. Saturated (NH₄)₂SO₄ was slowly added to a final concentration of 19 % (v/v) and the solution was mixed for 30 min at room temperature prior to centrifugation for 10 min at 2,000 \times g. Repetition of this precipitation step resulted in a HMW fibrinogen pellet (~99 % purity), which were dissolved in 5 mL of saline (0.9 % NaCl) and then dialysed against M199 culture medium, as was the UNF fibrinogen. Purity was determined using standard non-reducing sodium dodecylsulphate polyacrylamide gel electrophoresis and concentrations were calculated using the molar extinction coefficient of fibrinogen (E1 % 280 nm for fibrinogen is 15.8). The preparations were stored in single-use aliquots at -80 °C until further use.

In a custom-made mould, the porous titanium implants were filled with 55 μ L of either HMW fibrinogen (2 mg/mL, HMW-Fb) or UNF fibrinogen (2 mg/mL, UNF-Fb) which were clotted with 0.5 IU/mL of thrombin (Global Siemens Healthcare, Erlangen, Germany) dissolved in a 4.5 mM calcium chloride buffer (Baxter, Utrecht, Netherlands) in a 8.5:1 ratio. HMW fibrin gels with BMP-2 (HWM-BMP-Fb) were made by adding 3 μ g BMP-2 (Shanghai Rebene Biomaterials Co., China) in 1 mM saline solution to the HWM fibrinogen solution before clotting. Prior to implantation, after clotting the fibrin-filled implants were wrapped in Parafilm® and incubated for 15–18 h at 6 °C to allow completion of fibrin gelling.

Scanning electron microscopy (SEM)

To determine filling efficacy and to characterise the structure of the fibrin networks polymerised from HMW and UNF fibrinogen, SEM was used as follows: implants were filled with fibrin gels and fixed in 3 % glutaraldehyde for 24 h and rinsed with sodium phosphate buffer (0.1 M, pH 7.2-7.4; Merck). Samples were then consecutively dehydrated in ascending alcohol concentrations (30, 50, 70 and 90 % v/v) with three final incubations in 100 % ethanol for 10 min each. Probes were critical-point-dried in liquid CO₂ and then sputtered with a 30 nm gold layer. Samples were analysed in FEI/Philips XL 30 FEG ESEM (Philips) in a high vacuum environment.

Load-bearing segmental bone defects

Critical-sized segmental bone defects were made in the femora of 40 male 16-weeks-old Wistar rats (446 ± 32 g). Rats were divided into four experimental groups receiving porous titanium implants filled with HMW-BMP-Fb, HMW-Fb and UNF-Fb or were left empty (empty). The Animal Ethics Committee of the Erasmus University approved the study and Dutch guidelines for care and use of laboratory animals were followed. Before surgery, rats received subcutaneous injections of antibiotics (enrofloxacin, 5 mg/kg body weight) and pain medication (buprenorphine, 0.05 mg/kg body weight). Surgery was performed aseptically under general anaesthesia (1-3.5 % isoflurane). The right femur was exposed through a lateral skin incision and separation of underlying fascia. Using three proximal and three distal screws, a 23 × 3 × 2 mm polyether ether ketone (PEEK) plate (RISystem, Davos Platz, Switzerland) was fixed to the femur anterolateral plane. Periosteum was removed over 8 mm of the mid-diaphyseal region before a 6 mm cortical bone segment was removed with a wire saw and a tailor-made saw guide. Subsequently, a porous titanium implant was implanted press-fit into the defect. Finally, fascia and skin were sutured. Subcutaneous injection of pain medication (buprenorphine, 0.05 mg/kg body weight) was given twice a day for the following three days. Rats were sacrificed after twelve weeks with an overdose of pentobarbital (200 mg/kg body weight).

μCT evaluation

Bone regeneration was measured by *in vivo* μCT scans (SkyScan 1076; Bruker micro-CT N.V., Kontich, Belgium) at four, eight and twelve weeks, and by *ex vivo* μCT scans on isolated grafted femora at the end of the experiment. Rats were kept under general anaesthesia (1-3.5 % isoflurane) during *in vivo* μCT scans at 35 μm resolution (95 kV, 105 μA current, 1.0 mm Al/0.25 mm Cu filter, and 0.75° rotation step, 14 min scan). *Ex vivo* μCT scans were acquired at 18 μm resolution (95 kV, 100 μA current, 1.0 mm Al/0.25 mm Cu filter, and 0.5° rotation step). μCT scan images were reconstructed using volumetric reconstruction software NRecon version 1.6.6 (Bruker micro-CT N.V., Kontich, Belgium).

Bone regeneration was expressed as bone volume (BV), which was measured at four specific regions: 1) total BV: the total volume of bone formed within the 6 mm defect;

2) porous BV: the bone formed inside the porous space of the titanium implants; 3) outer BV: the bone formed outside the porous titanium implants; and 4) inner BV: the bone formed in the medullary canal of the implants. BV values were measured using CTAnalyser version 1.13 (Bruker micro-CT N.V., Kontich, Belgium). First the specific region was selected, then the titanium and its border artefacts was excluded from images using a global threshold with a value between titanium and bone and removal of an extra 35 μm border (size of one pixel) surrounding the titanium. Subsequently the bone was extracted by using a second global threshold that differentiated between bone and soft tissue. The global threshold values were chosen on visual inspection and were kept constant for all scans. Bone bridging was assessed on *ex vivo* scans with DataViewer 1.4 (Bruker micro-CT N.V., Kontich, Belgium). Complete bone bridging was defined as bridging of three or more cortices counted on *ex vivo* scans in the coronal and sagittal plane. Bone bridging was quantified by measuring the shortest remaining gap size between bone formed at the proximal and distal site of the 6 mm bone defect.

Histological evaluation

Histology was performed on two femora per group that represented the mean of the whole group. To select these two femora, all ten grafted femora were sorted according to their total BV after twelve weeks and the two femora closest to the averaged value were chosen. Harvested femora were fixed in 10 % neutral buffered formalin solution for two days, dehydrated in ascending alcohol concentrations (70 to 100 % v/v), and finally embedded in methyl methacrylate (MMA). Sections of ~20 μm were obtained using a diamond saw (Leica SP1600, Rijswijk, The Netherlands) and stained with basic fuchsin 0.3 % (w/v) solution and methylene blue 1 % (w/v) solution to stain bone purple and fibrous tissue blue, respectively. Serial sections were then screened for bone formation, bone-implant contact and bone bridging.

Biomechanical tests

Mechanical strengths of grafted femora were measured by a torsion test conducted on the remaining eight femora of each group. Three contralateral femora, serving as a reference of intact femora, were included as controls. After harvesting the femora, soft tissues and PEEK plates were carefully removed. Specimens were kept in 10 % neutral buffered formalin solution for two days, minimising the effects of formalin conservation on mechanical properties (Unger *et al.*, 2010), and then transferred to phosphate buffered saline. Subsequently, both ends of each femur were embedded in a cold-cured epoxy resin (Technovit 4071, Heraeus Kulzer, Germany). On the upper clamping side, a Cardan joint was used to ensure pure rotation without bending. The lower sides were simply fixed. Tests were performed until failure with a rotation rate of 0.5° s⁻¹ using a static mechanical testing machine that could apply a maximum torque of 450 N.mm (Zwick GmbH, Ulm, Germany). Torsional strength (maximum torque to failure, N.mm) was determined.

Statistics

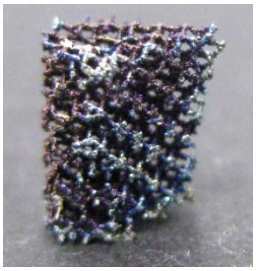
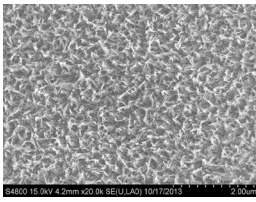
Statistical analyses were performed using SPSS Statistics 20.0 (SPSS, Inc.). Data are presented as means with standard deviations. One-way analysis of variation (ANOVA) and subsequent *post hoc* pairwise comparisons with Bonferroni adjustment were used to test for differences between the four groups. A power calculation (β -value > 0.80, SD ~ 25 %) was made to find a true difference in total BV of at least 35 %. Based on this calculation, $n = 10$ was required. $A p < 0.05$ was considered statistically significant.

Results

Porous titanium implants incorporated with fibrin gels

Porous titanium implants were produced using SLM in the anatomical shape of the surgically removed cortical bone segment (Fig. 1a). The implants had a porosity of 85 % and a pore size ranging from 460-670 μm (Table 1). The alkali-acid-heat treatment resulted in a titanium oxide layer with an irregular nano-scale features (Table 1). Macroscopic inspection and SEM analyses verified that the pores of the titanium implants were completely filled with fibrin gel (Fig. 1a-b). The protein fibres of both fibrin gels attached intimately to the surface-treated titanium (Fig. 1c). In addition, SEM showed clear differences between HMW-Fb and UNF-Fb gels with respect to their nanofiber structures: as compared to the fibre network formed by unfractionated fibrinogen, resulting in a much denser structures with smaller average pore diameters and

Table 1. Properties of porous titanium implants (Amin Yavari *et al.*, 2014b; Van der Stok *et al.*, 2013a).

Titanium implant	
Titanium thickness	165 \pm 43 μm
Pore size	577 \pm 146 μm (range 460-670 μm)
Porosity	85 %
Pore volume	55 mm^3
Compression strength	14 MPa
Young's modulus	0.4 GPa
Surface area / volume	0.034 μm^2
Surface composition	Oxygen 35 % Titanium 60 % Vanadium 2 % Aluminium 3 %
Surface topography (SEM)	

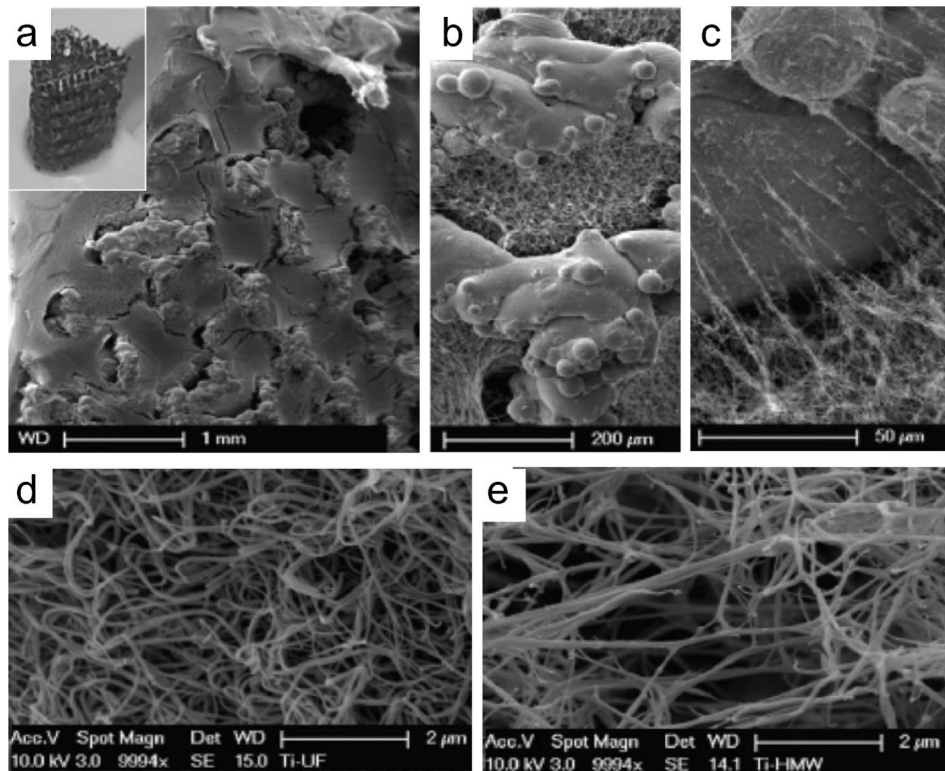


Fig. 1. SEM images of fibrin loaded porous titanium implants. Macroscopic overview, and enlarged details, of a fully fibrin-filled implant (a, b). The fibrin fibres are tightly bound to the implant surface (c). The fibre network resulting from unfractionated fibrinogen is rather dense with thin fibres (d). The fibrin network from HMW fibrinogen reveals a more-open, better-permeable, structure with slightly thicker fibres (e).

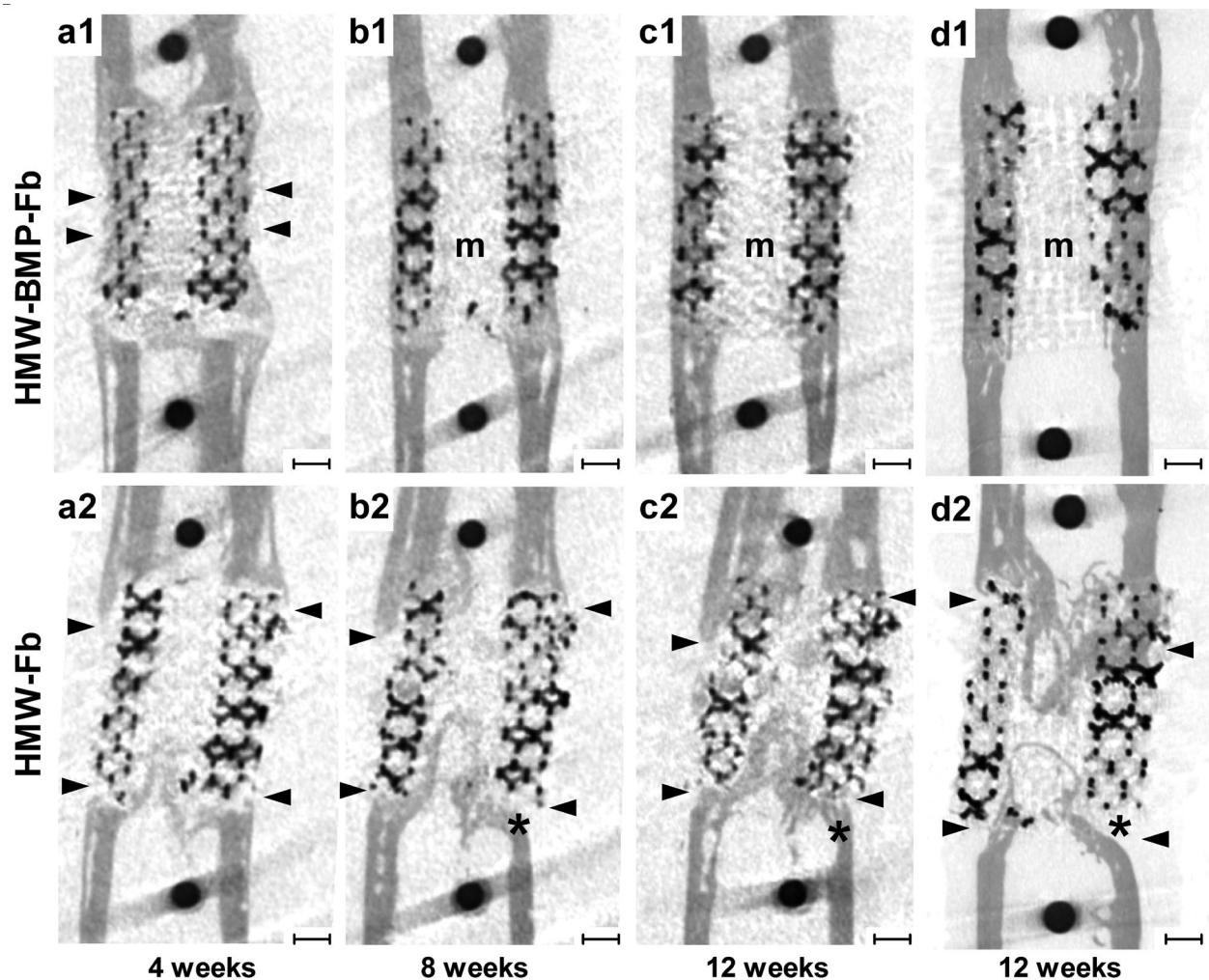


Fig. 2. Representative longitudinal μ CT scans illustrating the bone regeneration process. *In vivo* scans of defects grafted with porous titanium implants incorporated with high molecular weight fibrin with BMP-2 (HMW-BMP-Fb group) and high molecular weight without BMP-2 (HMW-Fb group) after four (a1-2), eight (b1-2) and twelve weeks (c1-2) as well as *ex vivo* after twelve weeks (d1-2). In the HMW-BMP-Fb group, rapid bone regeneration throughout the complete length of the defect is already observed after four weeks (a1, arrows). Between eight and twelve weeks, the cortex and medullary canal (indicated by 'm') are restored in their original shape (b1, c1, and d1). In the HMW-Fb group, bone regeneration is only observed at the proximal and distal side of the porous implants (a2, arrows); this bone is predominantly situated in the medullary canal and insufficiently bridging the defect (d2). Distally from the titanium implants, bone resorption is observed between eight and twelve weeks (asterisk). Bar indicates 1 mm.

thinner fibres (Fig. 1d), polymerisation of high molecular weight fibrinogen appeared to form a more open network with relatively thicker fibres (Fig. 1e).

Load-bearing segmental bone defects

All rats were able to tolerate weight-bearing activities immediately after surgery; the implantation sites healed without complications and all animals remained healthy during the follow-up.

μ CT evaluation

Porous titanium implants with HMW-BMP-Fb gels effectively stimulated bone regeneration (Fig. 2). Within four weeks, bone regeneration had occurred throughout the entire length of the porous titanium implants and after eight weeks, bridging of the defect was complete.

Only minimal bone regeneration was observed in those defects grafted with HMW-Fb containing porous titanium implants and consequently failed to bridge (Fig. 2). The load-bearing segmental defects grafted with HMW-BMP-Fb containing porous titanium implants fully restored the original bone architecture after twelve weeks (Fig. 2 and 3). Incorporation of HMW-Fb or UNF-Fb did not seem to outperform the empty porous titanium implants (Fig. 3).

Quantitative analysis of regenerated bone, based on *in vivo* μ CT scans, showed that the total BVs of the HMW-BMP-Fb group increased at each time point and reached an average of $65.1 \pm 14.9 \text{ mm}^3$ after twelve weeks (Fig. 4a). This was significantly higher than all the three control groups. Neither the total BV of the HMW-Fb ($37.7 \pm 26.4 \text{ mm}^3$) group nor that of the UNF-Fb ($32.1 \pm 13.4 \text{ mm}^3$) group was significantly different from

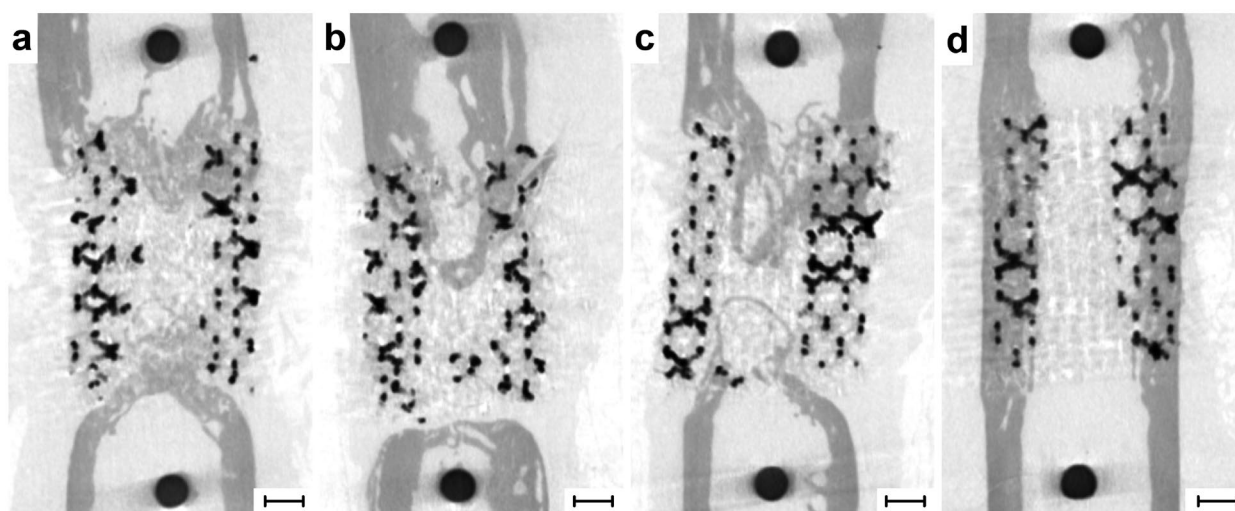


Fig. 3. Representative transversal *ex vivo* μ CT images of grafted segmental femur defects. Titanium implants and fixation screws appear in black, whereas bone appears in dark grey. In the empty (a), UNF-Fb (b) and HMW-Fb (c) groups; bone regeneration is predominantly seen at the proximal and distal third of the porous titanium implants. Some new bone has formed inside the porous implants, but most of the newly formed bone is seen in the medullary canal. In the HMW-BMP-Fb group (d), bone regeneration extended throughout the entire porous titanium implants, bridging the defect. Bone formed inside the porous implant, and no bone has been formed inside the medullary canal. Black bar indicates 1 mm.

the total BV of the empty group ($33.7 \pm 16.8 \text{ mm}^3$) (Fig. 4a). Also, the porous BV and outer BV of the HMW-BMP-Fb group were significantly higher than that of all three control groups (Fig. 4b-c). After twelve weeks, $51 \pm 8 \%$ of the available pore space of the titanium implants with HMW-BMP-Fb gels was filled with regenerated bone, twice as much as in the HMW-Fb ($24 \pm 18 \%$) and UNF-Fb ($21 \pm 5 \%$) group, respectively. The inner BV of the HMW-BMP-Fb group ($3.9 \pm 1.6 \text{ mm}^3$) significantly increased as compared to the control groups after four weeks. Contrary to the HMW-Fb and UNF-Fb groups, the inner BV of the HMW-BMP-Fb decreased over time ($3.1 \pm 1.3 \text{ mm}^3$ at 8 weeks and $2.6 \pm 1.3 \text{ mm}^3$ at 12 weeks) and even became significantly less than in the inner BV of the HMW-Fb group (Fig. 4d).

Bone bridging, determined on *ex vivo* μ CT scans at twelve weeks, was only seen in the cortical defects grafted with porous titanium implants filled with HMW-BMP-Fb gels (Fig. 5). Seven defects were completely bridged, and the average remaining gap size in the three defects that were not bridged was $0.8 \pm 0.1 \text{ mm}$ (Fig. 6a). The remaining gap size in the other three experimental groups was $1.8 \pm 1.6 \text{ mm}$ (HMW-Fb group), $1.9 \pm 0.9 \text{ mm}$ (UNF-Fb group) and $1.8 \pm 1.4 \text{ mm}$ (empty group), respectively.

Histological evaluation

Bone quality, assessed using light microscopy, showed that in the HMW-BMP-Fb group bone was formed almost exclusively at the site of the original cortex and an intimate contact between the regenerated bone and the titanium implant was found throughout the entire length of the defect (Fig. 7d vs. a-c). In the HMW-Fb (Fig. 7c), UNF-Fb (Fig. 7b) and empty groups (Fig. 7a), bone formation

occurred predominantly at the distal and proximal sites of the titanium implants that were close to the adjacent cortical bone. This bone formation never extended throughout the entire length of the porous implant. The remaining gaps in the defects were rather filled with amorphous fibrous tissue (Fig. 7a, b, and c). Strikingly, in the HMW-BMP-Fb group an open medullary canal was observed after twelve weeks (Fig. 7d), whereas in all control groups bone formation was blocking the medullary canal (Fig. 7a-c).

Biomechanical evaluation

Femora of the HMW-BMP-Fb group reached a significantly higher maximum torque than the three control groups (Fig. 6b). The specimens were more than twice as strong as control femora (248 %) and six femora of this HMW-BMP-Fb group were able to resist the maximum torque (450 N.mm) without breaking. Femora of the HMW-Fb group did not differ in maximum torque from the femora of the UNF-Fb or empty group. The average maximum torques were 60 % (HMW-Fb group, $86 \pm 29 \text{ N.mm}$), 51 % (UNF-Fb group, $75 \pm 20 \text{ N.mm}$), and 53 % (empty group, $77 \pm 53 \text{ N.mm}$), respectively, of the average maximum torque measured for control femora ($146 \pm 19 \text{ N.mm}$) (Fig. 6b).

Discussion

An ideal biomaterial, that can be used as a bone graft substitute, should be able to fully regenerate and bridge load-bearing segmental bone defects within a short period of time (Langer and Vacanti, 1993). Our combination of surface-treated porous titanium with BMP-2 containing

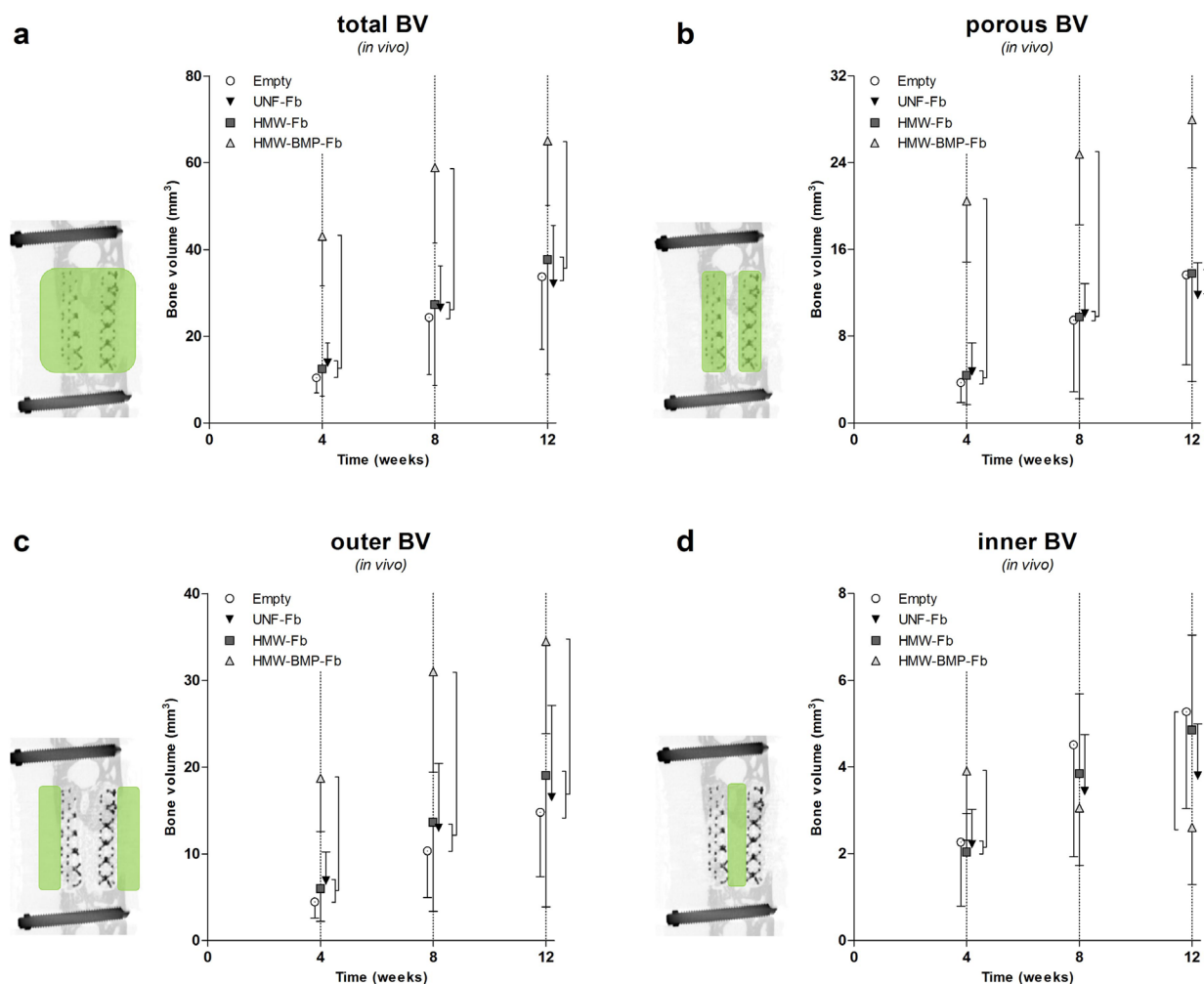


Fig. 4. Longitudinal quantification of bone regeneration. *In vivo* μ CT scans after four, eight and twelve weeks; total BV (**a**); defined as all bone formed within the 6 mm defect. Outer BV (**b**), defined as bone formed outside the titanium implants. Porous BV (**c**), defined as bone formed inside the porous space of the titanium implants. Inner BV (**d**), defined as bone formed in the medullary canal of the titanium implants. Values are expressed as mean and SD ($n = 10$ per group), and a one-way ANOVA test followed by a *post-hoc* Bonferroni correction was performed to test for statistical significant difference at each time point; $p < 0.05$ was considered as statistically significant, vertical bars indicate the significant differences found between the groups.

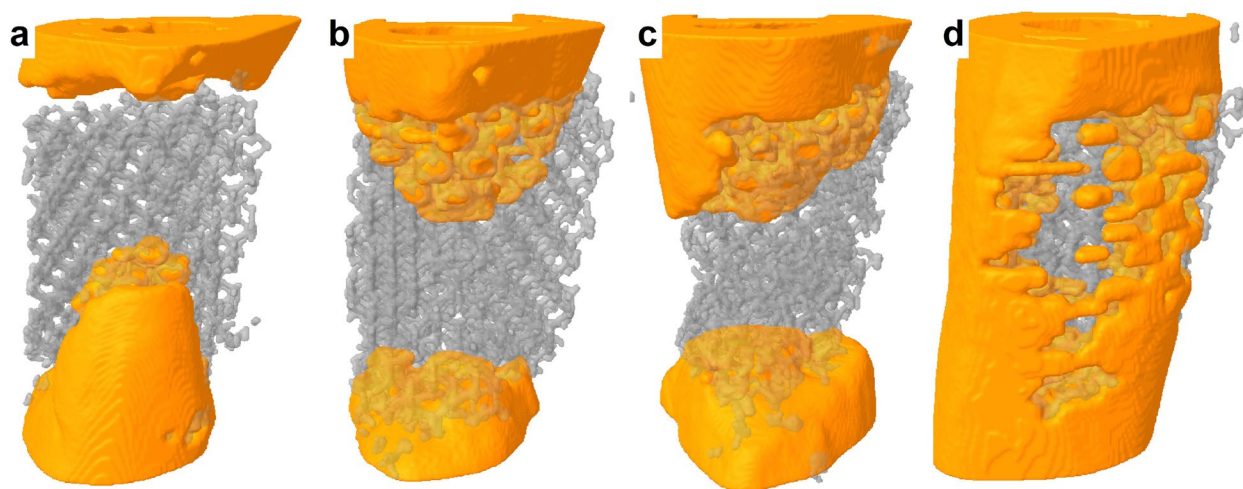


Fig. 5. Illustration of bone bridging. Representative 3D μ CT images showing the average extend of bone bridging of the empty (**a**), UNF-Fb (**b**), HMW-Fb (**c**), as well as the HMW-BMP-Fb (**d**) group. Porous titanium implants appear in transparent grey, whereas bone appears in yellow/dark grey.

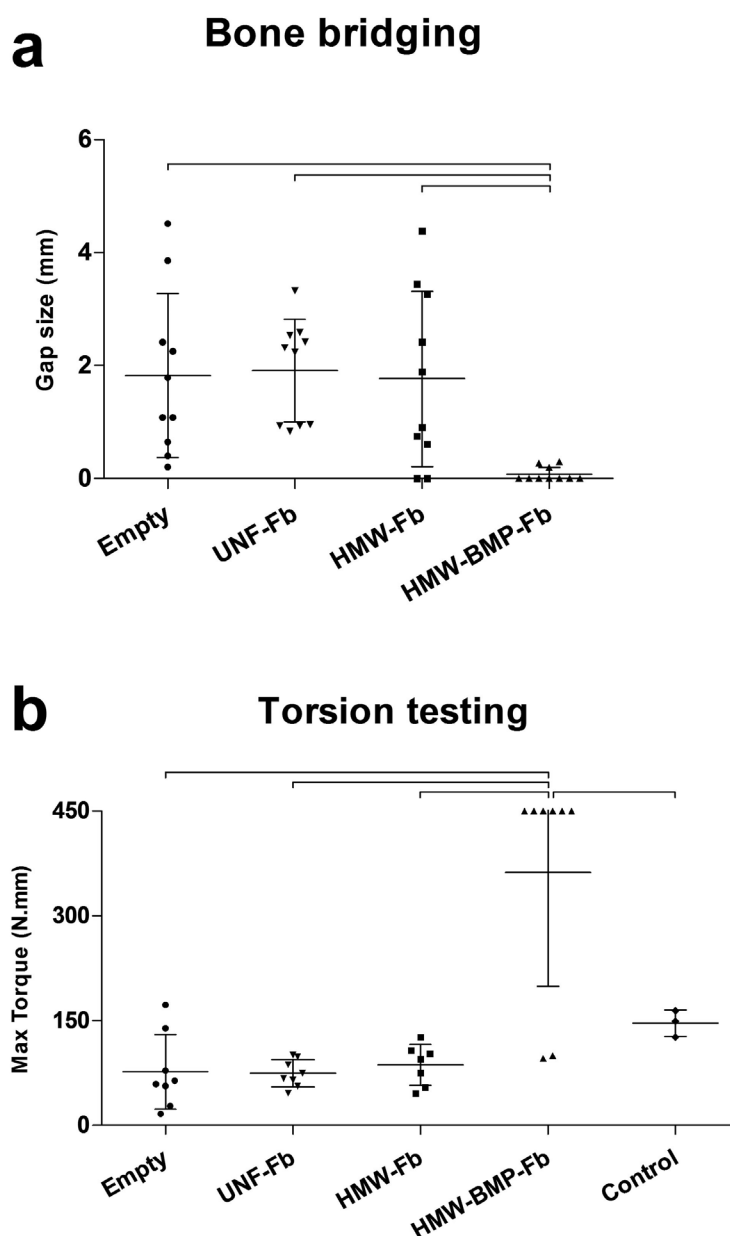


Fig. 6. Bone bridging and mechanical strength. The remaining gap size after twelve weeks was used to indicate bridging success (**a**). Mechanical femoral strength after implantation of porous titanium implants measured by torsion testing (**b**). As a positive control, three control femora were included to provide a reference of a normal strength of femora during torsion testing (**b**, control). Values are expressed as mean and SD, and a one-way ANOVA test followed by a *post-hoc* Bonferroni correction was performed to test for statistical significant differences at each time point; $p < 0.05$ was considered as statistically significant, horizontal bars indicate significant differences between groups.

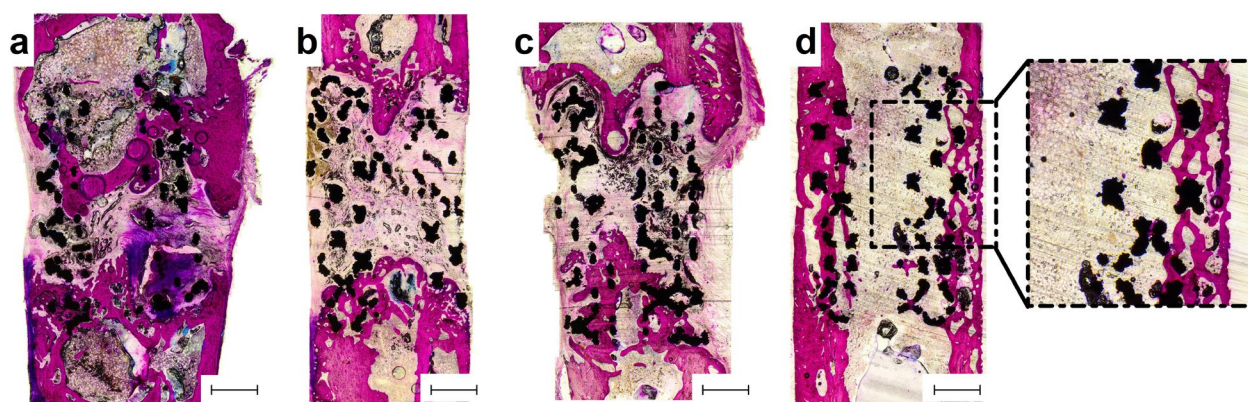


Fig. 7. Histological evaluation of bone bridging. Representative transversal sections of femur defects twelve weeks after implantation of porous titanium implants; empty (**a**), or incorporated with UNF-Fb (**b**), HMW-Fb (**c**) or HMW-BMP-Fb gels (**d**). Magnification reveals re-colonisation of the medulla with small round-shaped cells of a typical bone marrow stroma appearance. Sections are stained with basic fuchsin and methylene blue. Basic fuchsin stains bone purple, methylene blue stains fibrous tissue blue. Black bar indicates 1 mm.

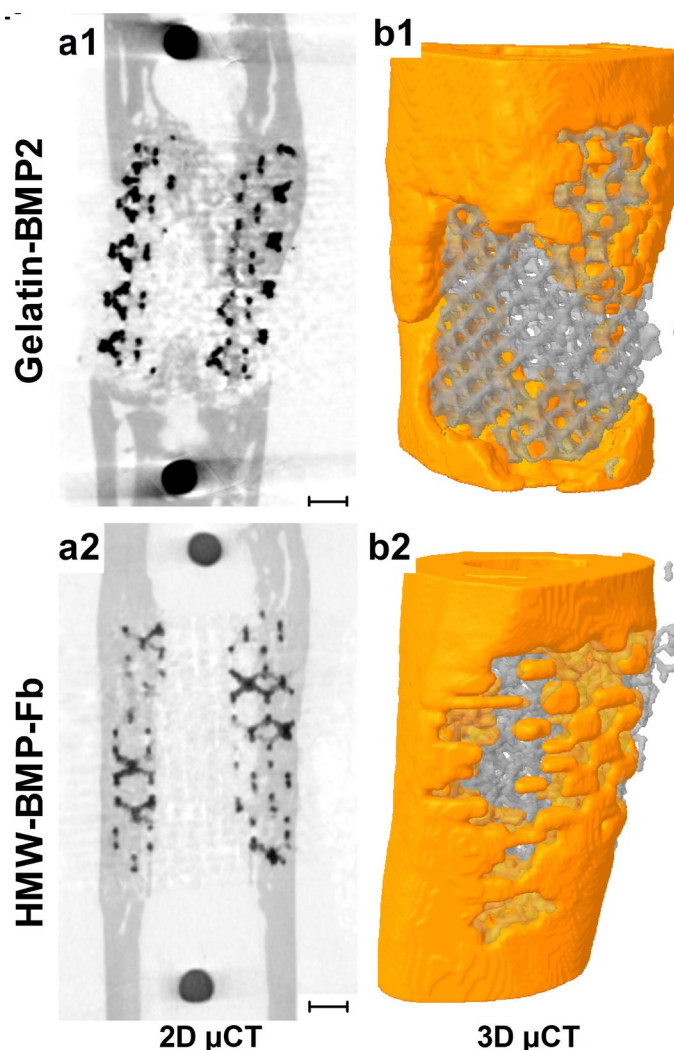


Fig. 8. Direct comparison between BMP-2 release from fibrin and gelatin on bone regeneration. In the same *in vivo* model, using the same type of porous titanium implants and same batch of BMP-2, results from using HMW-BMP-Fb gels (this work) or gelatin nanosphere gels (Van der Stok *et al.*, 2013b) were compared. Using gelatin nanosphere gels loaded with 3 μ g BMP-2 predominantly led to bone regeneration outside or inside the porous titanium implants (**a1**) without bridging the entire defect (**b1**). In contrast, HMW-BMP-Fb gels (loaded with the same dose of BMP-2) led to complete bridging with restoration of the medullary canal (**a2**) and the cortex (**b2**). Bar indicates 1 mm.

physiologically concentrated fibrin gels fully regenerated segmental bone defects in rat femora (Fig. 2 and 5) and fully recovered their mechanical strength (Fig. 6). Moreover, combining osteoconductive titanium with an osteoinductive BMP-2 releasing fibrin gel resulted in “guided” bone regeneration; *i.e.* new bone was formed throughout the porous titanium implants (Fig. 2) to specifically restore the cortex to its native anatomical shape as well as the medullary canal (Fig. 3 and 7d).

Biomaterials used for load-bearing segmental defects should offer sufficient support to withstand mechanical loading (Giannoudis *et al.*, 2011). A material with such mechanical properties is titanium, and solid titanium implants have been very successfully used in trauma and orthopaedic surgery over the past decades (Learmonth *et al.*, 2007). However, the notable biomechanical mismatch between solid titanium implants and surrounding bone frequently leads to stress-shielding, subsequent bone resorption and implant loosening (Niinomi, 2008). This limitation can be overcome by using mechanically optimised porous titanium implants (Murr *et al.*, 2011; Ryan *et al.*, 2009), the development of which greatly benefited from the introduction of additive manufacturing techniques. Techniques such as selective laser melting

(Hollander *et al.*, 2006; Mullen *et al.*, 2009; Stamp *et al.*, 2009), electron beam melting (EBM) (Heinl *et al.*, 2008; Hrabec *et al.*, 2011; Ponader *et al.*, 2010) or similar additive manufacturing techniques (Bandyopadhyay *et al.*, 2010; Bandyopadhyay *et al.*, 2009) allow for a personalised, anatomical implant design and control of its structural and mechanical properties alike. Our SLM-based, femur-shaped implants possessed mechanical properties within the physiological range of the host bone, while its fully interconnected porous structure is considered to be within the range required for osteoconduction (Table 1) (Van der Stok *et al.*, 2013a). Furthermore, the fatigue properties of the porous implants indicate that the biomechanical support is temporary (Amin Yavari *et al.*, 2013). The implants were therefore capable of offering sufficient mechanical support *in vivo*, while stimulating bone regeneration through osteoconduction in the segmental bone defects (Van der Stok *et al.*, 2013a; Van der Stok *et al.*, 2013b).

In addition to mechanical support, biomaterials should also offer a surface that facilitates osseointegration, *i.e.* intimate apposition of bone matrix onto the implant surface (Puleo and Nanci, 1999). The bone-implant interface of most metallic biomaterials including titanium usually consists of an interfacial fibrous-like layer (also called

laminae limitantes) (Puleo and Nanci, 1999). The formation of this fibrous-like layer can be avoided by relatively simple treatments that have been shown to improve osseointegration of solid titanium implants (Wennerberg and Albrektsson, 2009). We optimised the treatment of the porous titanium implants used in this study (Amin Yavari *et al.*, 2014b), to not only improve apatite formation and cellular attachment, but also cell proliferation and osteogenic differentiation of osteoprogenitor cells (Amin Yavari *et al.*, 2014b).

Bone graft substitutes should also be able to induce bone regeneration, which can be induced by a variety of bone morphogenetic proteins (BMPs), including BMP-2 and BMP-7 (Groeneveld and Burger, 2000). BMP-2 is mainly released during the first few days of the natural bone regeneration process, and BMP-7 plays a more important role during the later phase (Gerstenfeld *et al.*, 2003). Both BMP-2 and BMP-7 received FDA-approval (Termaat *et al.*, 2005), but their use in humans is currently heavily debated (Carragee *et al.*, 2011). Although the osteoinductive effect of BMP-2 has been demonstrated in a wide variety of species (including rats, rabbits, dogs, sheep and non-human primates) (An and Friedman, 1999), it is often argued that one must be cautious in assuming that stromal cells from other species may serve as models for inducible osteogenesis in human marrow stromal cells (Diefenderfer *et al.*, 2003). BMP-induced side effects, including cyst-like bone formation and soft tissue swelling, are likely caused by supra-physiological dosages used in humans (Carragee *et al.*, 2011) and these adverse effects were recently reproduced in a similar *in vivo* model as used in this study with BMP-2 concentrations exceeding 20 µg per defect (Angle *et al.*, 2012; Zara *et al.*, 2011). In contrast, a dose between 2.5 and 10 µg was found to be safe and effective for various other BMP release systems including alginate-based (Boerckel *et al.*, 2011), poly-L-lactic acid (PLLA)-based (Wei *et al.*, 2007) or silk-based (Bessa *et al.*, 2010) scaffolds. Based on these results we used 3 µg BMP-2 per implant. Furthermore, Schmoekel *et al.* demonstrated that with less soluble nonglycosylated BMP-2, the required cytokine dose could even be further reduced (Schmoekel *et al.*, 2004).

Surface-treated porous titanium was loaded with BMP-2 through incorporation in physiologically concentrated fibrin gels. This is different from fibrin gels that have been used in trauma and orthopaedic surgery as “fibrin glue”, as these sealants are made of highly supra-physiological fibrinogen concentrations (Janmey *et al.*, 2009). This supra-physiological concentration (50–100 mg/L) ensures quick and effective clotting, and is therefore primarily used as a haemostatic agent. Supra-physiological fibrinogen concentrations were also used to deliver BMP-2 in several bone defect models (Chung *et al.*, 2007; Kaipel *et al.*, 2012; Kim *et al.*, 2008; Koo *et al.*, 2013; Koo *et al.*, 2012; La *et al.*, 2012; Schmoekel *et al.*, 2004; Schmoekel *et al.*, 2004; Schutzenberger *et al.*, 2012; Yang *et al.*, 2010; Yang *et al.*, 2012). Schutzenberger *et al.* showed that fibrin gels outperformed the currently clinically used absorbable collagen sponges as BMP-release properties of fibrin, in contrast to those of collagen, allow to use 85 % less

cytokine without compromising the regenerative success (Schutzenberger *et al.*, 2012). However, the high fibrinogen concentration of these supra-physiological concentrated fibrin glues have a limiting effect on cell mobility and ingrowth (Nürnberg *et al.*, 2010; Peterbauer-Scherb *et al.*, 2012). *In vivo*, fibrin constitutes only 0.25 % of the volume of a blood clot (Weisel, 2004), which was mimicked in the current study by preparing fibrin gels of physiological concentrations (2–4 mg/L). It is tempting to speculate that at these concentrations, fibrin fibres form a more open network that more effectively promoted cell migration and cell ingrowth (Seebach *et al.*, 2014). This open network structure and fibrin fibre adherence was perfectly supported by the surface-treated porous titanium (Fig. 1c). This temporary fibrin network is not expected to remain intact *in vivo* for more than a few days (Schmoekel *et al.*, 2004), but the results obtained in this study suggest that this is sufficient to adequately induce bone regeneration. Our approach mimics physiological fracture healing, during which BMP-2 is entrapped in the spontaneously formed fracture haematoma to induce differentiation of mesenchymal stem cells into osteoblasts (Onishi *et al.*, 1998). These osteoblasts subsequently start to produce more BMP-2 and other important osteogenic cytokines to reach a maximum activity after 4–7 days (Kirker-Head, 1995).

Physiologically concentrated fibrin gels prepared from HMW fibrinogen were expected to improve bone regeneration, as compared to gels prepared from UNF fibrinogen, because HMW fibrinogen has been shown to promote angiogenesis *in vitro* and *in vivo* in our earlier studies (Kaijzel *et al.*, 2006). UNF fibrin gels contain 30 % low molecular weight fibrinogen and, compared to 100 % HMW fibrinogen, contamination with more than 10 % of LMW fibrinogen gradually decreased the formation of tube-like structure *in vitro* in a dose-dependent manner (Kaijzel *et al.*, 2006). However, implants with HMW-Fb gels alone did not enhance bone regeneration and performed similar to implants with UNF-Fb gels or empty porous titanium implants (Fig. 2 and 5). BMP-2 release from the fibrin gel is apparently providing the only osteoinductive stimulus, while HMW-Fb may still improve cell migration and angiogenesis. Whether using HMW-Fb to release BMP-2 is better than using UNF-Fb cannot be answered here and is a limitation of our study. However, HMW-fibrin gels with BMP-2 clearly outperformed previously used gelatin-based nanosphere gels with BMP-2 (Van der Stok *et al.*, 2013b), indicating the type of BMP-2 carrier is of crucial importance. Although gelatin gels were capable of a sustained release of BMP-2 (Wang *et al.*, 2013), this resulted in bone regeneration that mainly occurred around and inside the porous titanium implants (Fig. 8, a1). In addition, bone regeneration in that study did not lead to bridging of the grafted defects within twelve weeks (Fig. 8, b1). The mechanical strength also reached up to only 50 % of the original strength in that study (Wang *et al.*, 2013). In contrast, physiological fibrin gels with low doses of BMP-2 boosted bone regeneration in the present study and completely bridged the majority of the grafted defects within four weeks (Fig. 8, b2), filling up more than 50 % of the porous volume of the titanium implants with

regenerated bone. Twelve weeks following the surgery, the grafted femora were already more than twice as strong as their original strength (*i.e.* control femora Fig. 6).

Conclusion

This study reports the development of a new biomaterial combination, capable of stimulating complete bone regeneration in load-bearing segmental defects in rat femora. This optimal combination enabled quick bone regeneration within four weeks and full restoration of the original bone functionality and anatomical shape in this pre-clinical model. Since all used methods have been used separately in trauma and orthopaedic surgery, this combination should be evaluated in a large animal model or a clinical trial and this might result in an efficient bone graft substitute to graft load-bearing segmental bone defects in trauma and orthopaedic surgery.

Acknowledgements

This research forms part of the Project P2.04 BONE-IP of the research program of the BioMedical Materials institute, co-funded by the Dutch Ministry of Economic Affairs and was supported by a grant from the Dutch government to The Netherlands Institute for Regenerative Medicine (NIRM, grant No. FES0908). This research project was further supported by the START-Program of the Faculty of Medicine, RWTH Aachen. Osteosynthesis & Trauma Care foundation is acknowledged for financial support (2011-HWJV).

References

Alvarez K, Nakajima H (2009) Metallic scaffolds for bone regeneration. *Materials* **2**: 790-832.

Amin Yavari S, Ahmadi SM, Van der Stok J, Wauthle R, Riemsdijk AC, Janssen M, Schrooten J, Weinans H, Zadpoor AA (2014a) Effects of bio-functionalizing surface treatments on the mechanical behavior of open porous titanium biomaterials. *J Mech Behav Biomed Mater* **36**:109-119.

Amin Yavari S, van der Stok J, Chai YC, Wauthle R, Tahmasebi Birgani Z, Habibovic P, Mulier M, Schrooten J, Weinans H, Zadpoor AA (2014b) Bone regeneration performance of surface-treated porous titanium. *Biomaterials* **35**: 6172-6181.

Amin Yavari S, Wauthle R, van der Stok J, Riemsdijk AC, Janssen M, Mulier M, Kruth JP, Schrooten J, Weinans H, Zadpoor AA (2013) Fatigue behavior of porous biomaterials manufactured using selective laser melting. *Mater Sci Eng C Mater Biol Appl* **33**: 4849-4858.

An YH, Friedman RJ (1999) Animal models in orthopaedic research. CRC Press, New York.

Angle SR, Sena K, Sumner DR, Virkus WW, Viridi AS (2012) Healing of rat femoral segmental defect with bone morphogenetic protein-2: a dose response study. *J Musculoskelet Neuronal Interact* **12**: 28-37.

Bandyopadhyay A, Espana F, Balla VK, Bose S, Ohgami Y, Davies NM (2010) Influence of porosity on mechanical properties and *in vivo* response of Ti6Al4V implants. *Acta Biomater* **6**: 1640-1648.

Bandyopadhyay A, Krishna BV, Xue W, Bose S (2009) Application of laser engineered net shaping (LENS) to manufacture porous and functionally graded structures for load bearing implants. *J Mater Sci Mater Med* **20 Suppl 1**: S29-34.

Banwart JC, Asher MA, Hassanein RS (1995) Iliac crest bone graft harvest donor site morbidity. A statistical evaluation. *Spine (Phila Pa 1976)* **20**: 1055-1060.

Bessa PC, Balmayor ER, Hartinger J, Zanon G, Dopler D, Meinel A, Banerjee A, Casal M, Redl H, Reis RL, van Griensven M (2010) Silk fibroin microparticles as carriers for delivery of human recombinant bone morphogenetic protein-2: *in vitro* and *in vivo* bioactivity. *Tissue Eng Part C Methods* **16**: 937-945.

Boerckel JD, Kolambkar YM, Dupont KM, Uhrig BA, Phelps EA, Stevens HY, Garcia AJ, Guldberg RE (2011) Effects of protein dose and delivery system on BMP-mediated bone regeneration. *Biomaterials* **32**: 5241-5251.

Carragee EJ, Hurwitz EL, Weiner BK (2011) A critical review of recombinant human bone morphogenetic protein-2 trials in spinal surgery: emerging safety concerns and lessons learned. *Spine J* **11**: 471-491.

Cho TJ, Gerstenfeld LC, Einhorn TA (2002) Differential temporal expression of members of the transforming growth factor beta superfamily during murine fracture healing. *J Bone Miner Res* **17**: 513-520.

Chung YI, Ahn KM, Jeon SH, Lee SY, Lee JH, Tae G (2007) Enhanced bone regeneration with BMP-2 loaded functional nanoparticle-hydrogel complex. *J Control Release* **121**: 91-99.

de Wild M, Schumacher R, Mayer K, Schkommodau E, Thoma D, Bredell M, Kruse Gujer A, Gratz KW, Weber FE (2013) Bone regeneration by the osteoconductivity of porous titanium implants manufactured by selective laser melting: a histological and micro computed tomography study in the rabbit. *Tissue Eng Part A* **19**: 2645-2654.

Diefenderfer DL, Osyczka AM, Garino JP, Leboy PS (2003) Regulation of BMP-induced transcription in cultured human bone marrow stromal cells. *J Bone Joint Surg Am* **85-A Suppl 3**: 19-28.

Einhorn TA (1995) Enhancement of fracture-healing. *J Bone Joint Surg Am* **77**: 940-956.

Gerstenfeld LC, Cullinane DM, Barnes GL, Graves DT, Einhorn TA (2003) Fracture healing as a post-natal developmental process: molecular, spatial, and temporal aspects of its regulation. *J Cell Biochem* **88**: 873-884.

Giannoudis PV, Chris Arts JJ, Schmidmaier G, Larsson S (2011) What should be the characteristics of the ideal bone graft substitute? *Injury* **42 Suppl 2**: S1-2.

Groeneveld EH, Burger EH (2000) Bone morphogenetic proteins in human bone regeneration. *Eur J Endocrinol* **142**: 9-21.

- Heinl P, Muller L, Korner C, Singer RF, Muller FA (2008) Cellular Ti-6Al-4V structures with interconnected macro porosity for bone implants fabricated by selective electron beam melting. *Acta Biomater* **4**: 1536-1544.
- Hollander DA, von Walter M, Wirtz T, Sellei R, Schmidt-Rohlfing B, Paar O, Erli HJ (2006) Structural, mechanical and *in vitro* characterization of individually structured Ti-6Al-4V produced by direct laser forming. *Biomaterials* **27**: 955-963.
- Holm B, Nilsen DW, Kierulf P, Godal HC (1985) Purification and characterization of 3 fibrinogens with different molecular weights obtained from normal human plasma. *Thromb Res* **37**: 165-176.
- Hrabe NW, Heinl P, Flinn B, Korner C, Bordia RK (2011) Compression-compression fatigue of selective electron beam melted cellular titanium (Ti-6Al-4V). *J Biomed Mater Res B Appl Biomater* **99**: 313-320.
- Janmey PA, Winer JP, Weisel JW (2009) Fibrin gels and their clinical and bioengineering applications. *J R Soc Interface* **6**: 1-10.
- Kaijzel EL, Koolwijk P, van Erck MG, van Hinsbergh VW, de Maat MP (2006) Molecular weight fibrinogen variants determine angiogenesis rate in a fibrin matrix *in vitro* and *in vivo*. *J Thromb Haemost* **4**: 1975-1981.
- Kaipel M, Schutzenberger S, Schultz A, Ferguson J, Slezak P, Morton TJ, Van Griensven M, Redl H (2012) BMP-2 but not VEGF or PDGF in fibrin matrix supports bone healing in a delayed-union rat model. *J Orthop Res* **30**: 1563-1569.
- Khan SN, Lane JM (2004) The use of recombinant human bone morphogenetic protein-2 (rhBMP-2) in orthopaedic applications. *Expert Opin Biol Ther* **4**: 741-748.
- Kim SS, Gwak SJ, Kim BS (2008) Orthotopic bone formation by implantation of apatite-coated poly(lactide-co-glycolide)/hydroxyapatite composite particulates and bone morphogenetic protein-2. *J Biomed Mater Res A* **87**: 245-253.
- Kirker-Head CA (1995) Recombinant bone morphogenetic proteins: novel substances for enhancing bone healing. *Vet Surg* **24**: 408-419.
- Koo KH, Lee JM, Ahn JM, Kim BS, La WG, Kim CS, Im GI (2013) Controlled delivery of low-dose bone morphogenetic protein-2 using heparin-conjugated fibrin in the posterolateral lumbar fusion of rabbits. *Artif Organs* **37**: 487-494.
- Koo KH, Yeo do H, Ahn JM, Kim BS, Kim CS, Im GI (2012) Lumbar posterolateral fusion using heparin-conjugated fibrin for sustained delivery of bone morphogenetic protein-2 in a rabbit model. *Artif Organs* **36**: 629-634.
- La WG, Kwon SH, Lee TJ, Yang HS, Park J, Kim BS (2012) The effect of the delivery carrier on the quality of bone formed *via* bone morphogenetic protein-2. *Artif Organs* **36**: 642-647.
- Langer R, Vacanti JP (1993) Tissue engineering. *Science* **260**: 920-926.
- Learmonth ID, Young C, Rorabeck C (2007) The operation of the century: total hip replacement. *Lancet* **370**: 1508-1519.
- Martino MM, Briquez PS, Ranga A, Lutolf MP, Hubbell JA (2013) Heparin-binding domain of fibrin(ogen) binds growth factors and promotes tissue repair when incorporated within a synthetic matrix. *Proc Natl Acad Sci U S A* **110**: 4563-4568.
- Milleret V, Tugulu S, Schlottig F, Hall H (2011) Alkali treatment of microrough titanium surfaces affects macrophage/monocyte adhesion, platelet activation and architecture of blood clot formation. *Eur Cell Mater* **21**: 430-444.
- Mullen L, Stamp RC, Brooks WK, Jones E, Sutcliffe CJ (2009) Selective Laser Melting: a regular unit cell approach for the manufacture of porous, titanium, bone in-growth constructs, suitable for orthopedic applications. *J Biomed Mater Res B Appl Biomater* **89**: 325-334.
- Murakami N, Saito N, Horiuchi H, Okada T, Nozaki K, Takaoka K (2002) Repair of segmental defects in rabbit humeri with titanium fiber mesh cylinders containing recombinant human bone morphogenetic protein-2 (rhBMP-2) and a synthetic polymer. *J Biomed Mater Res* **62**: 169-174.
- Murr LE, Amato KN, Li SJ, Tian YX, Cheng XY, Gaytan SM, Martinez E, Shindo PW, Medina F, Wicker RB (2011) Microstructure and mechanical properties of open-cellular biomaterials prototypes for total knee replacement implants fabricated by electron beam melting. *J Mech Behav Biomed Mater* **4**: 1396-1411.
- Murr LE, Gaytan SM, Medina F, Lopez H, Martinez E, Machado BI, Hernandez DH, Martinez L, Lopez MI, Wicker RB, Bracke J (2010) Next-generation biomedical implants using additive manufacturing of complex, cellular and functional mesh arrays. *Philos Trans A Math Phys Eng Sci* **368**: 1999-2032.
- Niinomi M (2008) Mechanical biocompatibilities of titanium alloys for biomedical applications. *J Mech Behav Biomed Mater* **1**: 30-42.
- Nürnberg S, Wolbank S, Peterbauer-Scherb A, Morton TJ, Feichtinger GA, Gugerell A, Meinel A, Labuda K, Bittner M, Pasterner W, Nikkila L, Gabriel C, van Griensven M, Redl H (2010) Properties and potential alternative applications in fibrin glue. In *Biological Adhesive Systems* Ed. J. von Byern and I. Grunwald, Springer, Wien, 237-259.
- Onishi T, Ishidou Y, Nagamine T, Yone K, Imamura T, Kato M, Sampath TK, ten Dijke P, Sakou T (1998) Distinct and overlapping patterns of localization of bone morphogenetic protein (BMP) family members and a BMP type II receptor during fracture healing in rats. *Bone* **22**: 605-612.
- Pape HC, Evans A, Kobbe P (2010) Autologous bone graft: properties and techniques. *J Orthop Trauma* **24 Suppl 1**: S36-40.
- Peterbauer-Scherb A, Danzer M, Gabriel C, van Griensven M, Redl H, Wolbank S (2012) *In vitro* adipogenesis of adipose-derived stem cells in 3D fibrin matrix of low component concentration. *J Tissue Eng Regen Med* **6**: 434-442.
- Ponader S, von Wilmsowsky C, Widenmayer M, Lutz R, Heinl P, Korner C, Singer RF, Nkenke E, Neukam FW, Schlegel KA (2010) *In vivo* performance of selective

electron beam-melted Ti-6Al-4V structures. *J Biomed Mater Res A* **92**: 56-62.

Puleo DA, Nanci A (1999) Understanding and controlling the bone-implant interface. *Biomaterials* **20**: 2311-2321.

Ryan G, McGarry P, Pandit A, Apatsidis D (2009) Analysis of the mechanical behavior of a titanium scaffold with a repeating unit-cell substructure. *J Biomed Mater Res B Appl Biomater* **90**: 894-906.

Ryan G, Pandit A, Apatsidis DP (2006) Fabrication methods of porous metals for use in orthopaedic applications. *Biomaterials* **27**: 2651-2670.

Schmoekel H, Schense JC, Weber FE, Gratz KW, Gnagi D, Muller R, Hubbell JA (2004) Bone healing in the rat and dog with nonglycosylated BMP-2 demonstrating low solubility in fibrin matrices. *J Orthop Res* **22**: 376-381.

Schmoekel HG, Weber FE, Seiler G, von Rechenberg B, Schense JC, Schawalder P, Hubbell J (2004) Treatment of nonunions with nonglycosylated recombinant human bone morphogenetic protein-2 delivered from a fibrin matrix. *Vet Surg* **33**: 112-118.

Schutzenberger S, Schultz A, Hausner T, Hopf R, Zanoni G, Morton T, Kropik K, van Griensven M, Redl H (2012) The optimal carrier for BMP-2: a comparison of collagen *versus* fibrin matrix. *Arch Orthop Trauma Surg* **132**: 1363-1370.

Seebach E, Freischmidt H, Holschbach J, Fellenberg J, Richter W (2014) Mesenchymal stroma cells trigger early attraction of M1 macrophages and endothelial cells into fibrin hydrogels, stimulating long bone healing without long-term engraftment. *Acta Biomater* **10**: 4730-4741.

Senta H, Park H, Bergeron E, Drevelle O, Fong D, Leblanc E, Cabana F, Roux S, Grenier G, Fauchoux N (2009) Cell responses to bone morphogenetic proteins and peptides derived from them: biomedical applications and limitations. *Cytokine Growth Factor Rev* **20**: 213-222.

Stamp R, Fox P, O'Neill W, Jones E, Sutcliffe C (2009) The development of a scanning strategy for the manufacture of porous biomaterials by selective laser melting. *J Mater Sci Mater Med* **20**: 1839-1848.

Termaat MF, Den Boer FC, Bakker FC, Patka P, Haarman HJ (2005) Bone morphogenetic proteins. Development and clinical efficacy in the treatment of fractures and bone defects. *J Bone Joint Surg Am* **87**: 1367-1378.

Unger S, Blauth M, Schmoelz W (2010) Effects of three different preservation methods on the mechanical properties of human and bovine cortical bone. *Bone* **47**: 1048-1053.

Urist MR (1965) Bone: formation by autoinduction. *Science* **150**: 893-899.

Van der Stok J, Van der Jagt OP, Amin Yavari S, De Haas MF, Waarsing JH, Jahr H, Van Lieshout EEM, Patka P, Verhaar JA, Zadpoor AA, Weinans H (2013a) Selective laser melting-produced porous titanium scaffolds regenerate bone in critical size cortical bone defects. *J Orthop Res* **31**: 792-799.

Van der Stok J, Wang H, Amin Yavari S, Siebelt M, Sandker M, Waarsing JH, Verhaar JA, Jahr H, Zadpoor AA, Leeuwenburgh SC, Weinans H (2013b) Enhanced bone regeneration of cortical segmental bone defects using

porous titanium scaffolds incorporated with colloidal gelatin gels for time- and dose-controlled delivery of dual growth factors. *Tissue Eng Part A* **19**: 23-24.

Wang H, Zou Q, Boerman OC, Nijhuis AW, Jansen JA, Li Y, Leeuwenburgh SC (2013) Combined delivery of BMP-2 and bFGF from nanostructured colloidal gelatin gels and its effect on bone regeneration *in vivo*. *J Control Release* **166**: 172-181.

Wei G, Jin Q, Giannobile WV, Ma PX (2007) The enhancement of osteogenesis by nano-fibrous scaffolds incorporating rhBMP-7 nanospheres. *Biomaterials* **28**: 2087-2096.

Weisel JW (2004) The mechanical properties of fibrin for basic scientists and clinicians. *Biophys Chem* **112**: 267-276.

Wennerberg A, Albrektsson T (2009) Effects of titanium surface topography on bone integration: a systematic review. *Clin Oral Implants Res* **20 Suppl 4**: 172-184.

Woo EJ (2013) Adverse events after recombinant human BMP2 in nonspinal orthopaedic procedures. *Clin Orthop Relat Res* **471**: 1707-1711.

Yang HS, La WG, Bhang SH, Jeon JY, Lee JH, Kim BS (2010) Heparin-conjugated fibrin as an injectable system for sustained delivery of bone morphogenetic protein-2. *Tissue Eng Part A* **16**: 1225-1233.

Yang HS, La WG, Cho YM, Shin W, Yeo GD, Kim BS (2012) Comparison between heparin-conjugated fibrin and collagen sponge as bone morphogenetic protein-2 carriers for bone regeneration. *Exp Mol Med* **44**: 350-355.

Zara JN, Siu RK, Zhang X, Shen J, Ngo R, Lee M, Li W, Chiang M, Chung J, Kwak J, Wu BM, Ting K, Soo C (2011) High doses of bone morphogenetic protein 2 induce structurally abnormal bone and inflammation *in vivo*. *Tissue Eng Part A* **17**: 1389-1399.

Discussion with Reviewers

Reviewer I: How can such an implant be fixed? In addition, can the fixation be integral part of the construct?

Authors: This is an intriguing question and obviously an important aspect of implant development. Because porous titanium implants are developed using selective laser melting (an additive manufacturing technique) options for screw or pin fixation can be completely integrated into the implant design. Examples of porous implants designs are more thoroughly described by Murr (Murr *et al*, 2010).

Reviewer II: When you look more than 12 weeks, may it be possible that the titanium mesh is impairing further bone formation as it is not degrading?

Authors: Bone formation would be impaired if implantation of the porous titanium implants result in a significant mechanical mismatch with the surrounding bone. This could cause stress shielding and subsequent bone resorption. However, extensive mechanical testing of the produced porous titanium indicated that due to fatigue the implants will lose some of their initial strength over time (Amin Yavari *et al*, 2013). This gradual weakening of the implants will avoid stress-shielding and is more likely

to stimulate bone formation rather than impairing bone formation. The main disadvantage of the fact that titanium implants do not degrade is the long-term risk of infection.

Reviewer III: Is this laboriously produced fibrin much better than commercially available material?

Authors: That may depend on the application. We have already shown that HMW-Fb stimulates angiogenesis *in*

vitro (Kaijzel *et al.*, 2006). As our commercial UNF-Fb does not behave much differently from HMW-Fb, with respect to bone bridging, we cannot clearly answer this for the present study. However, our novel combination of a fibrin gel within a highly porous titanium implant results in very good bone regeneration – at least when using HMW-Fb with low doses of BMP-2. The limitations of this study are now thoroughly addressed.